Title

Influence of synoptic weather events on the isotopic composition of atmospheric moisture in a coastal city of the western United States

Journal

Water Resources Research, 49(6)

ISSN

00431397

Authors

Farlin, James
Lai, Chun-Ta
Yoshimura, Kei

Publication Date

2013-06-01

DOI

10.1002/wrcr.20305

Peer reviewed

WATER RESOURCES RESEARCH, VOL. 49, 3685–3696, doi:10.1002/wrcr.20305, 2013

Influence of synoptic weather events on the isotopic composition of atmospheric moisture in a coastal city of the western United States

James Farlin,[1,2] Chun-Ta Lai,[1] and Kei Yoshimura[3]

Received 29 December 2012; revised 12 April 2013; accepted 7 May 2013; published 21 June 2013.

[1] Synoptic weather events are known to strongly influence the isotope composition of precipitation in continental locations. In this study, we present hourly values of water vapor isotopologues (HDO and $H_2{}^{18}O$) measured over a 30 day period in locally extreme weather conditions, including Santa Ana winds and winter rainstorms, in San Diego, California, USA. We investigate how atmospheric and hydrological processes influence HDO and $H_2{}^{18}O$ using an isotope-enabled GCM model (IsoGSM). Combining measurements and IsoGSM simulation, we demonstrate that convective mixing of marine and continental air masses are responsible for the isotopic variation of near-surface water vapor in this coastal location. The isotopic variability is most pronounced during Santa Ana winds. The Santa Ana winds represent a unique boundary layer condition in which atmospheric mixing becomes the process that dominantly controls the changes in the isotopic composition relative to air humidity. We demonstrate that a two-source mixing approach (Keeling plot) can reliably be used to estimate the isotopic composition of the source moisture, and from that, to infer the location of the moisture origin that contributes to the atmospheric moisture content in southern California. The present study is unique because it combines large-scale isotope GCM modeling with a robust and high-resolution isotope data set to disentangle the control of atmospheric and hydrologic processes on the atmospheric humidity in an extratropical climate. Our results demonstrate the utility of using single-point, ground-based isotope observations as a complementary resource to existing satellite isotope measurements for constraining isotope-enabled GCMs in future investigation of atmospheric water cycle.

Citation: Farlin, J., C.-T. Lai, and K. Yoshimura (2013), Influence of synoptic weather events on the isotopic composition of atmospheric moisture in a coastal city of the western United States, *Water Resour. Res.*, *49*, 3685–3696, doi:10.1002/wrcr.20305.

1. Introduction

[2] Stable isotopes have long been used to trace the major processes that affect the hydrologic cycle [*Craig*, 1961]. Understanding the origin and movement of water vapor provides insight into the global hydrologic cycle [*Gat*, 1996]. Much of the progress made in understanding the isotopic composition of atmospheric water has been limited to collecting and analyzing the isotopic composition of precipitation [*Araguas-Araguas et al*., 2000; *Kendall and Coplen*, 2001; *Rozanski et al*., 1992]. Previous work focused on surface water [*Kendall and Coplen*, 2001] and precipitation [*Berkelhammer et al*., 2012; *Buenning et al*., 2012; *Ciais and Jouzel*, 1994; *Jouzel et al*., 1997; *Merlivat and Jouzel*, 1979] to characterize local meteoric water lines that generalize combined effects of many hydrological processes taking place over multiple temporal and spatial scales. However, precipitation collection is often too coarse to analyze changes within a synoptic event [*Bowen and Wilkinson*, 2002]. This is because the isotopic signature of precipitation reflects the net effect of many processes, namely, thermodynamic equilibrium, diffusive transfer associated with evaporation and condensation, and atmospheric mixing of moisture sources, that all contribute to the variability in the isotopic composition of precipitation [*Barras and Simmonds*, 2009; *Dansgaard*, 1964]. Knowledge regarding isotope variations in water vapor is needed to decipher the relative contribution of each of these primary processes that combine to determine the isotopic composition of precipitated waters.

[3] Characterizing the mechanisms controlling isotope variability of atmospheric moisture has not been possible without model simulation due to a dearth of direct observations [*Yoshimura et al*., 2008]. Isotope-enabled GCMs were developed to investigate forcing mechanisms in the water cycle that alter water vapor isotopologues, and in turn, to inform climate models of the atmospheric and hydrologic processes that act as the primary control of moisture sources, transport, and distribution [*Brown et al*., 2008; *Hoffmann et al*., 1998; *Jouzel et al*., 1987; *Noone*, 2012;

[1]Department of Biology, San Diego State University, San Diego, California, USA.
[2]Graduate Group in Ecology, University of California Davis, Davis, California, USA.
[3]Atmosphere and Ocean Research Institute, The University of Tokyo, Kashiwa, Chiba, Japan.

Corresponding author: C.-T. Lai, Department of Biology, San Diego State University, 5500 Campanile Drive, San Diego, CA 92182, USA. (chun-ta.lai@mail.sdsu.edu)

0043-1397/13/10.1002/wrcr.20305

Risi et al., 2008a; *Schneider et al*., 2010; *Yoshimura et al*., 2008, 2011]. Ensemble statistical analyses from isotope-enabled GCMs simulations [e.g., *Brown et al*., 2008; *Noone*, 2012] are a powerful approach to depict the history of exchange processes giving rise to the isotopic composition of water vapor [*Payne et al*., 2007; *Risi et al*., 2008a, 2008b; *Sayres et al*., 2010; *Worden et al*., 2007; *Wright et al*., 2009; *Yoshimura et al*., 2011]. A critical component to the knowledge gained from these modeling exercises resides in the realism of model simulation when compared to actual observations. Satellite-based isotope measurements, such as those from Tropospheric Emission Spectrometer [TES, *Worden et al*., 2007] and the Scanning Imaging Absorption Spectrometer for Atmospheric Chartography [SCIAMACHY, *Frankenberg et al*., 2009], have been used to validate atmospheric boundary layer integrated isotope GCM simulation but with limited success. This is because of the inherent uncertainties associated with the satellite data [*Brown et al*., 2008; *Noone*, 2012; *Worden et al*., 2011; *Yoshimura et al*., 2011]. Ground-based observations are becoming a growing source of water vapor isotope data that complement satellite-based measurements to constrain GCM simulations.

[4] New laser spectroscopy instrumentation allows reliable and frequent isotope data acquisition for investigating mechanisms that control the variation of water vapor isotopologues at a variety of temporal scales. To date a number of research groups have demonstrated the capability of commercially available laser water isotope analyzers for in situ water vapor isotopologue measurements [*Lee et al*., 2005; *Wen et al*., 2008; *Sturm and Knohl*, 2010; *Gupta et al*., 2009; *Rambo et al*., 2011; *Good et al*., 2012]. Ground-based laser isotope analyzers have been deployed to estimate bias in the TES isotope measurements [*Worden et al*., 2011], to investigate synoptic weather influences on air mixing in the subtropics [*Noone et al*., 2011] and the effect of evapotranspiration on the water vapor isotope variation in plant canopies [*Griffis et al*., 2010; *Lee et al*., 2007; *Welp et al*., 2008]. Nevertheless, continuous isotopic measurements of water vapor remain sparse. To our best knowledge, observations that encompass synoptic weather cycles and extreme weather events have not been reported.

[5] Synoptic weather circulation has been shown to strongly influence the isotope composition of precipitation and atmospheric moisture measured in continental locations [*Berkelhammer et al*., 2012; *Buenning et al*., 2012; *Lai et al*., *2006*; *Lee et al*., 2006; *Risi et al*., 2010; *Schneider et al*., 2010; *Wen et al*., 2010; *Yoshimura et al*., 2008, 2010; *Zhang et al*., 2011]. Recent studies that employed statistical downscaling (isotope-enabled regional climate models (RCMs)) to optimize the parameterization of subgrid processes showed improved agreement between observed and modeled isotopic variations [*Yoshimura et al*., 2010, *Pfahl et al*., 2012]. This modeling technique has the potential to deliver new information with respect to subgrid hydrological processes that control water balance on the catchment scale, but this potential is critically tied to the training of the model's skills to simulate observed isotopic variability.

[6] The objectives of this study are to first report observed temporal variations in the isotopic composition of near-surface water vapor in a coastal city of southern California, USA. This unique data set presents hourly values of water vapor isotopologues (HDO and $H_2{}^{18}O$) measured over a 30 day period in locally extreme weather conditions, including Santa Ana winds and winter rainstorms, in February of 2011. These isotope observations were independently analyzed to deduce the origin of source moisture. We simulate atmospheric moisture transport and investigate how local atmospheric and hydrological processes influence the isotopic composition of near-surface water vapor using an isotope-enabled GCM model [IsoGSM, *Yoshimura et al*., 2008]. The nudged IsoGSM simulation was able to capture the rapid transition in the observed isotopic variation triggered by synoptic weather events. Combining observations and IsoGSM simulation, we investigate the dominant atmospheric processes that affect the isotopic composition of water vapor in locally extreme weather conditions.

2. Methods

2.1. Study Site and General Weather Conditions

[7] Isotopic variation in atmospheric water vapor was measured on the campus of San Diego State University (32.775°N and 117.072°W, elevation 136 m, 18.5 km east from the Pacific Ocean) in San Diego, California, USA. Warm dry summers and mild winters characterize the Mediterranean climate for this region. Precipitation occurs mostly between November and April. The long-term average annual precipitation is 250 mm with high seasonal and interannual variability [*Pavia and Badan*, 1998]. The mean air temperature is 14°C and mean precipitation 60 mm for the month of February.

[8] Our sampling location's geographic proximity to the Pacific Ocean and Anza-Borrego Desert creates an opportunity to observe and investigate synoptic weather controls on the loading and isotopic variation of atmospheric moisture. The prevailing oceanic breezes along with sporadic winter rainstorms presumably supply the primary inputs of atmospheric moisture to the region. This region is subject to the influence of Santa Ana winds. Santa Ana conditions are characterized by a strong pressure gradient between high-pressure subsidence systems in the Great Basin and the coast of Southern California [*Hughes and Hall*, 2010]. Under Santa Ana conditions, easterly wind of high velocity and low humidity prevails that temporarily creates an extreme weather condition conducive to wildfire. Rapid and drastic changes in air humidity and temperature often occur under the influence of Santa Ana winds [*Hughes and Hall*, 2010].

[9] Weather data reported in this study were collected in the nearby Montgomery Field airport (32.811°N and 117.141°W). During our study period, we observed two types of locally extreme weather events: Santa Ana conditions (Figure 1, periods A and B) and winter rainstorms. Santa Ana conditions were identified here as periods when relative humidity drops below the historic mean minimum value (Figure 1, red dashed line). On this basis, we identified two periods of Santa Ana winds that first occurred between DOY 33 and 34 (Episode A), and again between DOY 41 and 44 (Episode B). Five isolated precipitation events (DOY 30, 32, 37, 47, and 49–51) occurred during the study period, with cumulative amounts ranging from 0.25 to 36.8 mm of rain for each single storm.

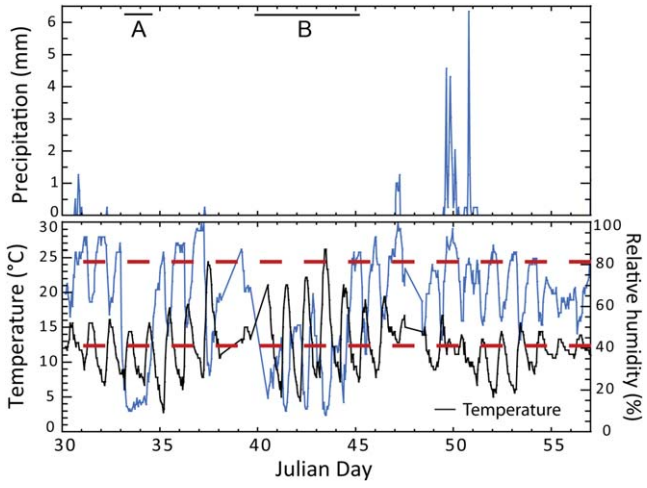

Figure 1. Meteorological conditions for the study period. Long-term mean maximum and minimum values of relative humidity coincided with the study period are also plotted (red dashed lines). Locally extreme weather conditions, including two Santa Ana wind periods (episodes A and B) and three larger winter rainstorms, were identified (see text).

2.2. Water Vapor Isotopologue Measurements and Analysis

[10] A Water Vapor Isotope Analyzer (model WVIA-24), commercially manufactured by Los Gatos Research (LGR Inc., Mountain View, CA, USA), operated in our laboratory to measure the near-surface atmospheric moisture content and its isotope composition from 30 January to 24 February 2011. A sample inlet was installed 1.5 m above a nonpermeable surface. Ambient air was drawn through 1/4″ polytetraflouroethylene (PTFE) tubing using an external diaphragm pump (KNF, N920AP.29.18) at a flow rate of 800 mL min^{-1}. This flow rate is sufficiently high enough to avoid lags in the instrument response time given that the total length of the sampling tube is only 3 m from the tip of the inlet to the analyzer for hourly averaging. Data were acquired at 2 Hz.

[11] The WVIA has been shown to reliably measure δD and δ^{18}O of water vapor only if operated with rigorous calibration at hourly intervals [*Rambo et al*., 2011; *Aemisegger et al*., 2012; *Kurita et al*., 2012]. We follow the calibration procedure described in *Rambo et al*. [2011] where more details can be found therein. Briefly, a Water Vapor Isotope Standard Source unit (WVISS, LGR Inc.) was coupled with the WVIA to perform online calibration once every hour. The WVISS uses a nebulizer to inject a miniscule water droplet from a large reservoir of reference water into a heated chamber, providing complete vaporization without fractionation of the reference water. In each calibration cycle, reference gases were introduced at three levels of H_2O mixing ratios encompassing the range of ambient H_2O mixing ratios in a way that the mixing ratio at the intermediate level closely resembles those in the ambient vapor. A new calibration curve was developed every hour to correct for raw readings recorded within the same hour. Corrected data were then averaged to yield highly accurate and precise δD and δ^{18}O values hourly.

[12] Figure 2 shows an example of the long-term performance of the system following the hourly calibration protocol as described in *Rambo et al*. [2011]. In this example, the vapor mixing ratio (VMR) of the reference gas was set to 10,000 ppmV, which resembles the typical atmospheric moisture content during our study period. Raw readings with no or poor calibration had first been excluded. Figure 2 shows that greater than 95% of the corrected data from this 30 day study period are accurate to within ±0.5‰ for δD and ±0.1‰ for δ^{18}O from the reference values. These data were used in further analyses.

2.3. Rain Water Collection and Analysis

[13] During precipitation events, rainwater was collected at hourly intervals when possible. A Petri dish was placed at ground level in an open area to capture rainwater. Hourly, the water from the Petri dish was collected and poured into scintillation vials, sealed with Parafilm and stored in the laboratory refrigerator until analysis.

[14] The isotope analysis of liquid water samples was performed on a DLT-100 Liquid Water Isotope Analyzer (LWIA, LGR Inc.) coupled to a LC PAL autosampler system (CTC Analytics AG, Zwingen, Switzerland) in the Ecosystem Ecology Lab at San Diego State University. An aliquot of 0.5 ml rainwater was loaded in a 2 ml sample vial for isotope analysis. Five laboratory working reference waters, selected on the basis to meet the expected range in the isotope ratio of sample waters, were included in each run to capture and correct for the instrument drift. Post data analysis was performed with LGR's LWIA data software. Our laboratory (Laboratory No. 110) received "A" grades for its participation on measuring blind water samples distributed by the IAEA 2011 proficiency test on the determination of stable isotope in water. The overall accuracy of liquid water isotope measurements is 0.1(±0.07) ‰ for δ^{18}O and 0.6(±0.4) ‰ for δD, respectively. Our day-to-day precision is reported as 0.25‰ for δ^{18}O and 1.0‰ for δD.

2.4. IsoGSM Simulation

[15] Isotope-enabled atmospheric general circulation models are useful for producing global water isotope field. IsoGSM is a modified NCEP/DOE Reanalysis (so-called NCEP Reanalysis 2) global spectral model (GSM) with water isotopes incorporated [*Yoshimura et al*., 2008]. Gaseous forms of heavier isotopologues of water (HDO and $H_2{}^{18}O$) were incorporated into the GSM as prognostic variables in addition to water vapor. The IsoGSM incorporates isotopic fractionation associated with precipitation process, allowing the stable isotope values to fluctuate with changing water vapor conditions (precipitation, condensation, and evaporation). Uniqueness of the IsoGSM is that it uses the global spectral nudging technique [*Yoshimura and Kanamitsu*, 2008] to describe prevailing wind conditions and provide greater insight into water isotope circulation patterns. IsoGSM is driven by observed atmospheric circulation (as opposed to sea surface temperature as being done in other models), thereby improving the agreement between observed and modeled isotope variations. IsoGSM has been used with TES data [*Worden et al*., 2007] to understand below cloud effects on the isotopic composition of precipitation and water vapor [*Lee et al*., 2011]. IsoGSM isotope simulations have been compared with both TES

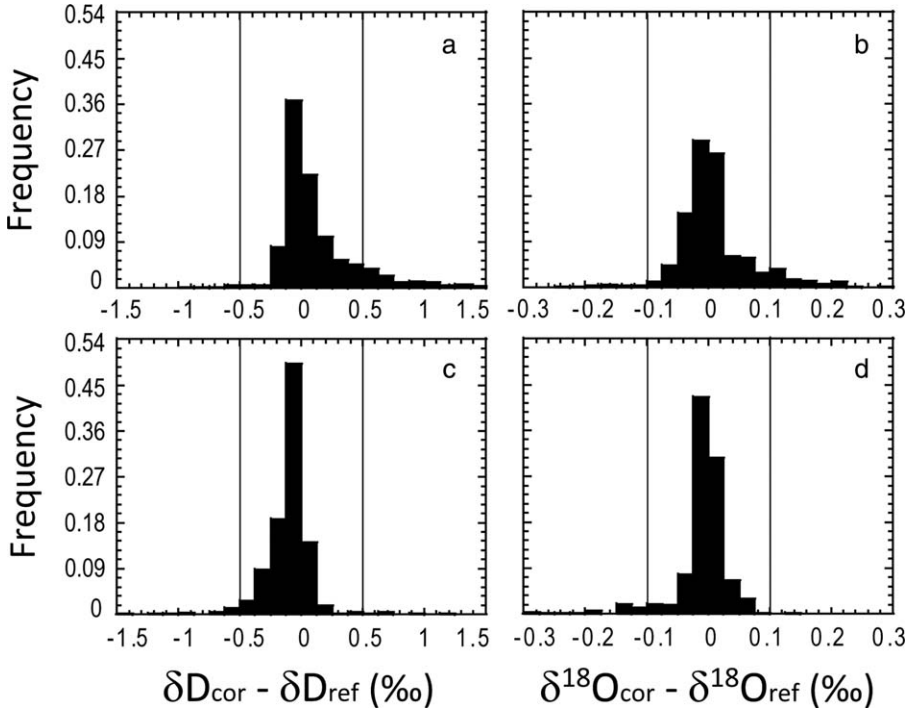

Figure 2. An example showing the accuracy of the water vapor δD and δ^{18}O data reported in this study. At H_2O mixing ratio = 5000 ppmV (a and b), greater than 88% of the corrected data (δ_{cor}) fall within the range of $\pm$0.5‰ for δD and $\pm$0.1‰ for δ^{18}O, respectively, when compared to the reference values (δ_{ref}). At mixing ratio = 10,000 ppmV (c and d), > 95% of the δ_{cor} values fall within the same range when compared to the δ_{ref} values.

[*Yoshimura et al*., 2011] and SCHIAMACHY [*Frankenberg et al*., 2009; *Yoshimura et al*., 2011] spectroscopic satellite isotope data. Discrepancies between model simulation and satellite-based isotope observations have been reported [*Yoshimura et al*., 2011]. However, the uncertainty in the satellite δD measurements remains large enough that they cannot be used to diagnose the potential shortcomings in the model. IsoGSM simulations have also been compared to ground-based isotope observations. For example, *Schneider et al*. [2010] investigated the IsoGSM's performance using isotope data acquired by a fourier transform infrared spectroscopy (FTIR) network. These authors reported that a large systematic discrepancy exists between observed and modeled amplitude in seasonal cycles of δD values. In this study, we continue these efforts of model-data comparison to further evaluate how IsoGSM simulates day-to-day δD and δ^{18}O variability of near-surface atmospheric water vapor under extreme weather conditions in a coastal city. The resolution of the model is T62, that is, about 180 km in horizontal and 28 levels in vertical resolution. IsoGSM describes the land surface process using the NOAH model [*Ek et al*., 2003]. The model assumes no isotopic fractionation of evapotranspiration fluxes from the land surface (i.e., assuming 100% transpiration).

3. Results and Discussion

[16] We begin by presenting the observed variability from hourly to synoptic scales in section 3.1. In section 3.2, we compare IsoGSM simulations with the continuous measurements before using IsoGSM to aid to the interpretation of the observed variability in the δ^{18}O and δD of near-surface water vapor. We investigate and find distinct isotope-mixing ratio relationships that differ between synoptic weather events, which enable us to differentiate atmospheric mixing from the condensation-driven processes that separately control the isotope variability in the near-surface water vapor. These results are discussed in section 3.3. In section 3.4, we demonstrate that Santa Ana winds represents a unique condition where changes in the atmospheric moisture content and its isotopologues can be explained by the mixing between two classes of air masses, that is, the moist marine vapor and the dry, tropospheric air that descends to the surface driven by a continental high pressure system. Finally, we estimate the isotopic composition of the source moisture using a two-source mixing approach. Using this information, we suggest that the advection of marine vapor of tropical origin provides a major supply to the atmospheric moisture in the coastal region of southern California.

3.1. Variability in the Observed Mixing Ratio and Isotopologues in Near-Surface Water Vapor

[17] Figure 3 shows the hourly averages of near-surface VMR, δ^{18}O, δD and deuterium excess [$d = \delta D - 8 \times \delta^{18}O$, *Dansgaard*, 1964] observed during the entire month of February in 2011. Observed isotope ratios ranged from $-$23.2‰ to $-$11.1‰ for δ^{18}O, $-$170.6‰ to $-$84.1‰ for δD, and $-$7.2‰ to 33.7‰ for d, respectively. Synoptic weather events depict large day-to-day variability with rapid transitions in the VMR and the isotope ratios usually

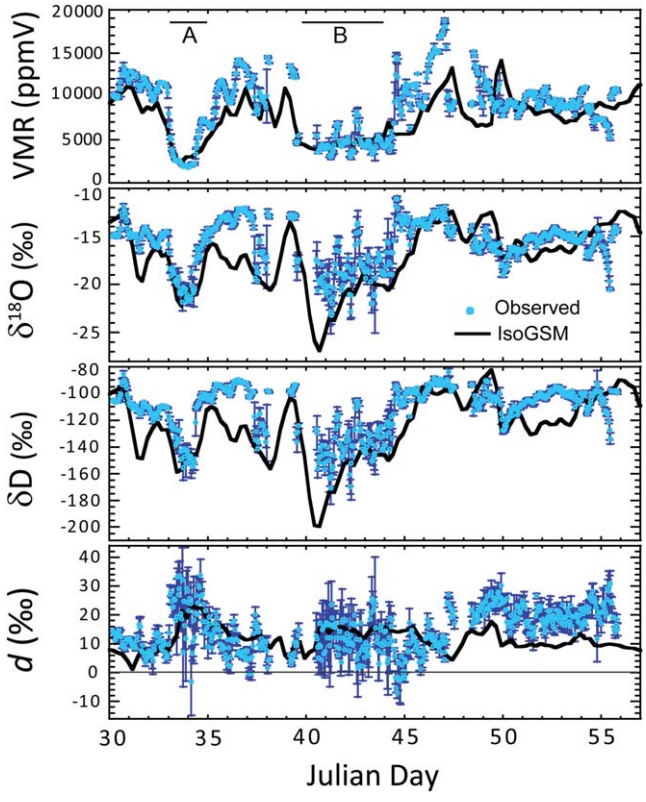

Figure 3. Time series of hourly observations in the vapor mixing ratio (VMR), water vapor $\delta^{18}O$, δD, and deuterium excess (d). The error bar represents 1 S.D. around the mean. Also shown is the IsoGSM simulation (solid lines). The two Santa Ana wind periods are marked as episode A and B.

correspond to the timing of these air masses moving in and out of San Diego. Two distinct periods of Santa Ana winds (episodes A and B) were characterized by remarkably low near-surface VMR (~2000 ppmV) along with a transition to much lower $\delta^{18}O$ and δD values under the strong influence of the synoptic event, followed by a rapid recovery to higher and more typical $\delta^{18}O$ and δD values as the Santa Ana wind subsided.

[18] *Rambo et al*. [2011] evaluated the performance of the WVIA for a variety of air moisture conditions. They reported that instrument stability declines as the air becomes substantially drier, which can be seen by the larger error bars in the $\delta^{18}O$ and δD values under Santa Ana winds. This instrument limitation may have increased the noise in the data but it does not deteriorate the accuracy (see Figure 2) and the robust pattern displayed by the continuous and high frequency measurements. On rainy days and in wet conditions, we observed relatively high $\delta^{18}O$ and δD values compared to drier conditions. At this time, we are not aware of any previous studies that have reported hourly measurements of water vapor isotope ratios observed under extreme weather conditions in the Mediterranean climate.

[19] With respect to synoptic variations in the d value of near-surface water vapor, we observed a rapid increase to the highest d values under the influence of the Santa Ana episode A period. This synoptic weather event occurred 2 days after a small rain event that resulted in a decent amount of rainfall (3.1 mm) for the area. Evaporation is known to increase d values in the vapor [*Gat*, 1996; *Lai and Ehleringer*, 2011]. The high d values observed during the Santa Ana episode A period likely reflect the highly evaporative condition (exceptionally low humidity but relatively wet surface) that removed a great deal of surface moisture at this time. By contrast, we did not observe elevated d values during the second Santa Ana period (episode B). The second Santa Ana event occurred a week after the first Santa Ana event and was not preceded by major rainfall, leading to insignificant surface evaporation despite low humidity. Following the two intensive rainstorms that occurred on DOY 47 and again, between DOY 49 and 51, d values increased by roughly 9‰ for an extended period (from an average of 10.3 ± 2.4‰ between DOY 41 and 47 to 19.7 ± 2.2‰ between DOY 53 and 59). These elevated d values in the vapor can be explained by the enhanced evaporative condition (wet surface). These results suggest that d values in near-surface water vapor are sensitive to surface wetness. Careful evaluations of the continuous d measurements may be useful for revealing landscape scale surface wetness and evaporative conditions.

3.2. IsoGSM Modeled Mixing Ratio and Isotopologues in Near-Surface Water Vapor

[20] Figure 3 also compares IsoGSM simulations with observations. IsoGSM reasonably captured the dynamic changes in VMR and water vapor isotopologue ratios during the rapid transitions of a synoptic weather cycle. Surprisingly, IsoGSM did very well reproducing the rapid and drastic fluctuations under the influence of Santa Ana winds. This agreement lends support to the quality of the data. IsoGSM simulates the timing of the precipitation very well, but tends to underestimate $\delta^{18}O$, δD, and d values during and following a rain event, suggesting that the model may not have adequately parameterized the condensation process taking place in the convective cloud [*Yoshimura et al*., 2011]. IsoGSM also failed to capture the shift in the d values after DOY 47 as revealed by the measurements. It should be noted that there is an inherent limitation in these comparisons as the two approaches represent processes that occur at different spatial scales. IsoGSM produces average values for the bottom level of the modeled atmosphere (the lowest 50 m of the air above the surface) but the observation was made at 1.5 m aboveground. In this study, IsoGSM simulations were evaluated with the large 200 km × 200 km grid size, which is far greater than the footprint of our measurements. These limitations would have resulted in systematic discrepancies rather than random errors as shown in Figure 3. Hence, there is real value in using ground-based observations to evaluate the performance of isotope-enabled GCMs.

[21] Next, we used IsoGSM to simulate spatial distribution of atmospheric moisture content and its isotopologues to investigate how large-scale atmospheric circulation could have explained the isotopic variation of near-surface water vapor during extreme weather events. Figure 4 illustrates the stark differences between two of the extreme weather events, with Figures 4a–4d corresponding to a Santa Ana event (episode B; at 16:00 on DOY 40) and

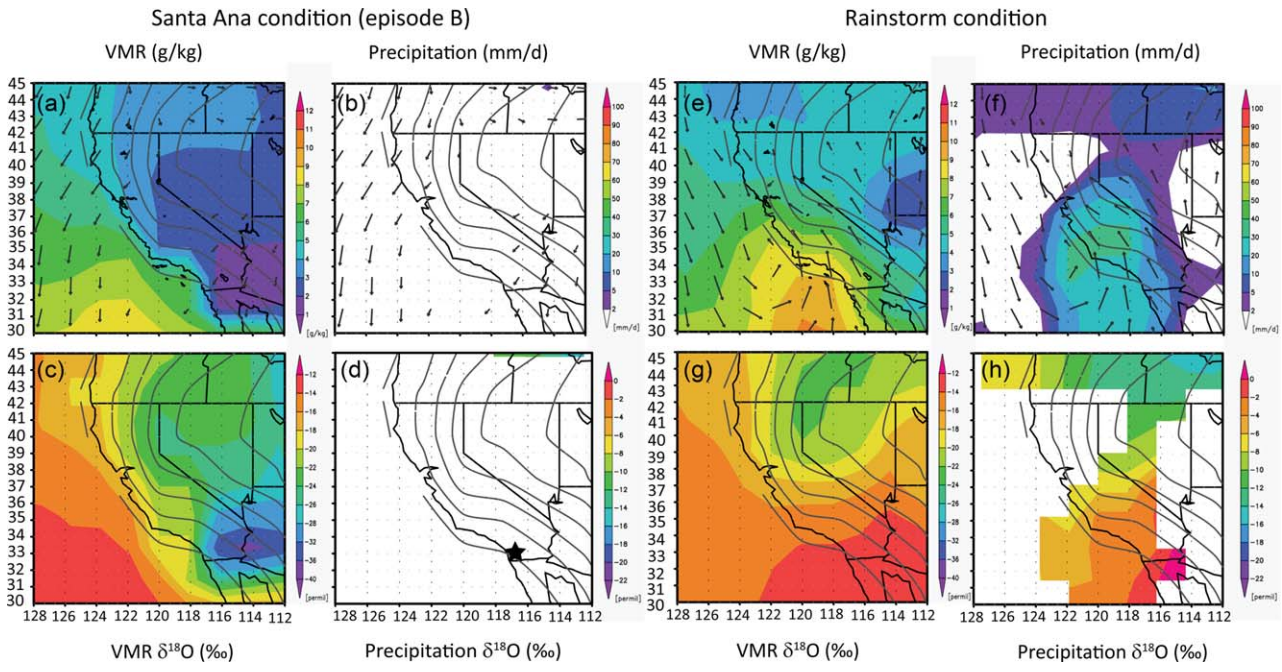

Figure 4. Examples of IsoGSM simulation for two extreme weather events. (a–d) A snapshot during the Santa Ana episode B period. (e–h) a snapshot during a rainstorm event occurring on DOY 50. Model outputs represent averages for the lowest level of the atmosphere in the IsoGSM (0–50 m above the surface).

Figures 4e–4h corresponding to a rainstorm event (at 16:00 on DOY 49). IsoGSM simulations show an air mass of very low VRM (Figure 4a) and very negative δ^{18}O values (Figure 4c) moving in the southwestern direction approaching the San Diego region. This continental air mass reduced near-surface air humidity to below average levels (Figure 1) that correspond with very negative vapor isotope ratios (Figure 3). By contrast, IsoGSM shows an air mass of high VMR (Figure 4e) with relatively enriched δ^{18}O (Figure 4g) that appeared to originate from the eastern tropical Pacific Ocean moving north through the region. This marine-based, moisture-loaded air mass resulted in significant rainfall (Figure 4f) with highly enriched δ^{18}O (Figure 4h). The impacts of these large-scale convective processes on the atmospheric humidity and isotopic composition are in general agreement with the findings with respect to the mesoscale control on the isotopic variation in precipitation for this region [*Berkelhammer et al*., 2012].

[22] To investigate how subgrid convection and mixing affects VMR and isotope composition in the atmospheric boundary layer (ABL), we used IsoGSM to simulate the vertical transfer of atmospheric moisture and its isotopologues. Figure 5 shows the modeled vertical gradient for the δ^{18}O of water vapor, along with information on air movement in the air column. Coinciding with Santa Ana wind periods (upper plot shaded boxes), strong subsidence transports air of low humidity and very low δ^{18}O values from the free troposphere, which then mixes with the relatively moist air in the ABL (lower plot). These modeling results suggest that the strong entrainment of tropospheric air creates a pronounced, yet short-lived, mixing event that rapidly and drastically alters the humidity and isotopic composition near the surface (upper plot). It should be noted that the entrained air into the ABL is ultra-dry. Its influence on the near-surface moisture budget should be interpreted as a "diluting" effect that reduces the moisture content by mixing into a relatively moist air mass in the lower ABL. The strong mixing between the entrained dry air mass and relatively moist surface air masses in the ABL is unique and only coincides with Santa Ana periods. Under the influence of prevailing low pressure systems (rainstorm events), strong convective transport moves surface air of high humidity and isotopic composition upward to dominate the vertical distribution in the ABL (see the upper plot in Figure 5 for days that are marked by blue arrows). These are also times when high humidity and higher δ^{18}O values were observed at the surface.

[23] Results presented here are consistent with the interpretation put forth by isotope tracer studies that focus on water cycles in the tropics [*Galewsky and Hurley*, 2010; *Noone et al*., 2011; *Risi et al*., 2008a; *Worden et al*., 2007]. Our results differ, however, because our observations were made by a single-point, ground-based instrumentation in an extratropical location as opposed to studies that incorporate satellite isotope data in the model comparison [*Brown et al*., 2008; *Frankenberg et al*., 2009; *Noone*, 2012; *Worden et al*., 2007; *Yoshimura et al*., 2011]. To further demonstrate the utility of near-surface isotope observations, we now turn to focus on exploiting the ground-based isotope measurements.

3.3. Observed δ-VMR Relationship and Its Diagnosis

[24] *Noone* [2012] described a theoretical framework for investigating atmospheric and hydrological processes that influence the relationship between mixing ratios and isotopic composition of water vapor. Changes in δ relative to

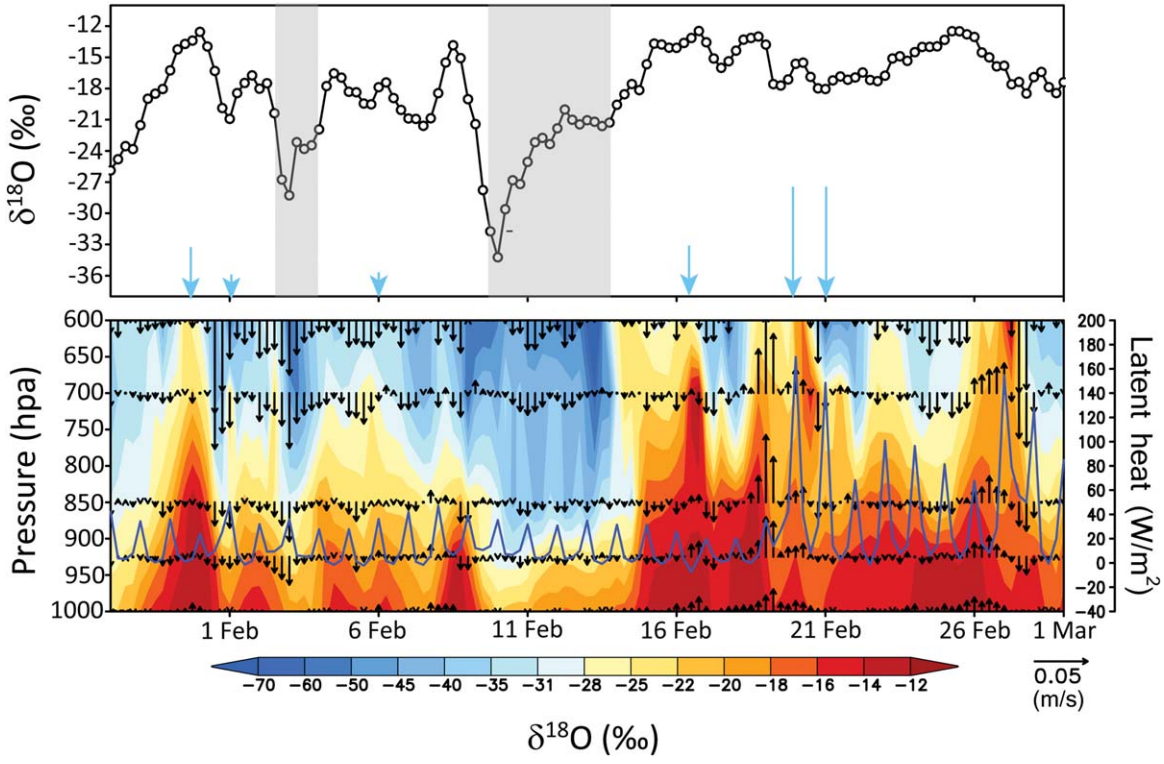

Figure 5. IsoGSM simulations for (upper) the time series of water vapor $\delta^{18}O$ near the surface (0–50 m) and (lower) the vertical profile of water vapor $\delta^{18}O$ in the air column. For the upper plot, the blue arrows indicate the timing of rainfall events whereas the gray boxes indicate the timing of Santa Ana winds. For the lower plot, the arrows indicate the direction of air movement in the column. The size of the arrow is scaled to the wind speed (m/s) whereas the blue curves indicate latent heat fluxes from the surface (W/m^2).

VMR are different for different processes [*Noone*, 2012]. By characterizing the δ-VMR relationship, one will gain knowledge regarding atmospheric/hydrologic controls over the abundance and transport of atmospheric moisture. Here we use hourly isotope and VMR measurements to examine these relationships derived under the influence of extreme weather conditions. We observed distinct patterns in the δ-VMR relationship between Santa Ana wind and rainstorm conditions. Measurements from the two Santa Ana periods (Figure 6, red and green circles) form distinct δ-VMR patterns that resemble those controlled by atmospheric mixing between two isotopically distinct air masses [isentropic, *Noone*, 2012]. The δ-VMR relationship observed during the first Santa Ana event (episode A) is clearly distinguishable from the second event (episode B) as the former representing a more extreme condition (drastic and rapid changes to lower VMR and isotope ratios). In each case, tropospheric air of very low VMR and isotope ratios descend to mix with relatively moist air near the surface (Figure 5). This descending motion compresses air that gives rise to warm temperature often recorded with the Santa Ana winds. A third mixing relationship appears to exist (the one that intersects with the lowest mixing curve). These data points coincide with a weak and short Santa Ana-like event that occurred on DOY 37 (Figures 1 and 2). Overall, atmospheric mixing between dry continental air and moist air masses, likely of marine origin, appears to be the dominant process controlling near-surface air humidity in the driest condition commonly known as Santa Ana winds for the region. Measurements during rainstorms show a δ-VMR relationship that forms a cluster of higher VMR and isotopic composition. The processes that often lead to this type of δ-VMR cluster have been described as Rayleigh or super-Rayleigh [*Noone*, 2012; *Yoshimura et al*., 2011].

[25] To further demonstrate the mixing process at work that blends dry continental air with marine moisture, we used IsoGSM to generate two δ-VMR relationships that coincide with two types of atmospheric humidity conditions. The first relationship (Figure 7b) describes the atmospheric humidity and δD in a modeled wet cell. A small portion of this model cell overlaps with the coastal area but the majority covers the ocean surface (i.e., west of our sampling location). The second relationship (Figure 7c) describes the atmospheric humidity and δD in a modeled dry cell that covers much of the land area over the Great Basin (i.e., east of our sampling location). The separation of wet and dry cells is a direct result of the spatial discretization in the model that reflects differences in surface properties and parameterization. Other researchers have discussed the importance of wet cell bias when comparing AGCM model data to land-based observations [*John and Soden*, 2007; *Schneider et al*., 2010]. The modeled wet cell shows high VMR and δD values that cluster over a relatively small range in the δ-VMR space (Figure 7b). The modeled dry cell shows VMR and δD values spanning over

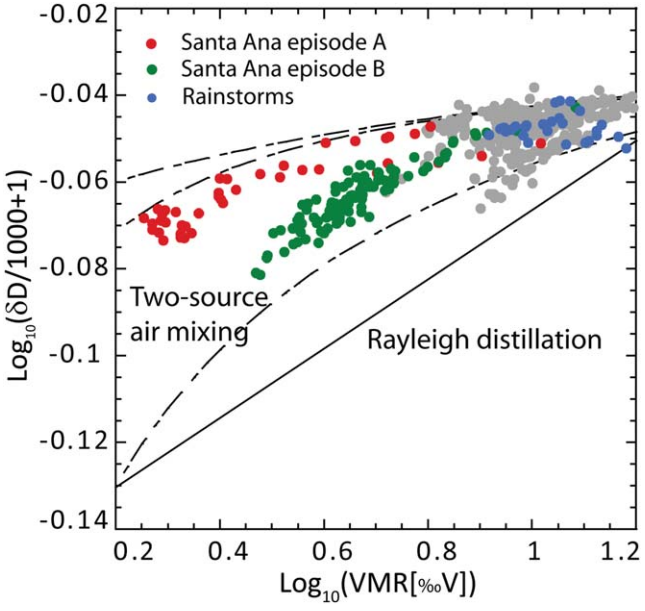

Figure 6. Relationships between vapor mixing ratio (VMR) and its isotopic composition (δD). The δ-VMR relationship is expressed on a log-log scale, in which, the Rayleigh process reduces to a simple linear fashion (solid line). An open system and a single temperature were assumed for describing the Rayleigh process. Observed δ-VMR relationships are illustrated in solid circles and differentiated by color. The three mixing lines (dashed curves) assume the mixing between a given dry air mass and a marine air mass of constant isotopic composition ($\delta D = -80‰$ for marine vapor). In this example, the three mixing lines are constructed by assuming three dry air masses of 0.6, 0.3, and 0.15‰V, respectively, along with a constant $\delta D = -350‰$.

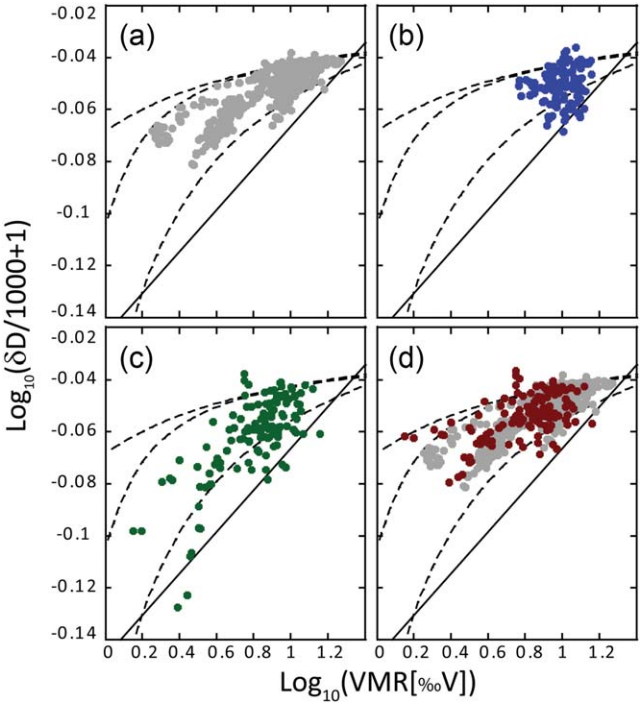

Figure 7. Comparison between IsoGSM and observed δD-VMR relationships as found in (a) measurements for the entire period, (b) a modeled wet cell, (c) a modeled dry cell, and (d) combined model cells weighted by the respective VMR in Figures 7b and 7c.

a greater space. These two model cells are adjacent to each other that combine to encompass the greater San Diego region. Considering either dry or wet cell alone fails to fully capture the observed δ-VMR relationships (Figure 7a) for the entire study period. By combining model predictions from the two cells using a VMR mass-weighted transfer function, the IsoGSM was able to reproduce the transient δ-VMR relationship for the entire month (Figure 7d) and overcome systemic wet/dry cell bias in the AGCM simulation as known previously [*Frankenberg et al*., 2009; *John and Soden*, 2007].

3.4. A Two-Source Mixing Approach for Identifying the Source of Atmospheric Moisture

[26] The two Santa Ana periods are great examples of times when atmospheric mixing becomes the process that dominantly controls the changes in the isotopic composition relative to air humidity. Under such idealized atmospheric condition, a two-source mixing approach [*Keeling*, 1958; *Noone*, 2012] can theoretically be used to identify the source of atmospheric moisture. The two-source mixing approach (i.e., Keeling plot) leads to a simple linear relationship when the reciprocal of VMR was plotted against the corresponding isotope ratios. The intercept of this linear relationship indicates the isotope composition of the source moisture [*Keeling*, 1958]. *Good et al*. [2012] show that the Keeling plot approach is robust when combined with high-temporal resolution data. We applied this approach by incorporating all the data points observed between DOY 40 and 45 (i.e., episode B) and showed the results in Figure 8. For this period, the approach yields robust results as evidenced by the high statistical significance. The intercepts of the mixing regression were $\delta^{18}O_{source} = -9.5$ (SE 0.2) ‰, $p < 0.0001$, $R^2 = 0.92$ and $\delta D_{source} = -75.5$ (SE 1.4) ‰, $p < 0.0001$, $R^2 = 0.93$, giving a ratio of $(\delta D/\delta^{18}O)_{source} = 7.95$ that suggests a source vapor in equilibrium with ocean waters. Furthermore, combining the values of the two intercepts results in an average d_{source} value = 0.5‰ for this period. This d value suggests that the kinetic effect is negligible during evaporation off the ocean surface, and that the vapor is close to be in equilibrium with ocean waters. This conclusion follows the notion that deuterium excess in water vapor over the ocean is mainly affected by sea surface temperature and relative humidity [*Masson-Delmotte et al*., 2005]. The combined observation between a ratio of $(\delta D/\delta^{18}O)_{source} = 7.95$ and a value of $d_{source} = 0.5‰$ also rules out precipitated waters as a potential major source of moisture to the atmosphere (via evapotranspiration), in that precipitated waters are subjected to both equilibrium and kinetic effects that lead to a globally averaged d value = 10‰, also known as the intercept in the global meteoric water line (GMWL). Indeed, the isotopic composition of precipitation sampled during our study period shows a range of d values from 7.3 to 31.7‰ (Table 1), substantially larger than the d_{source} value inferred from the

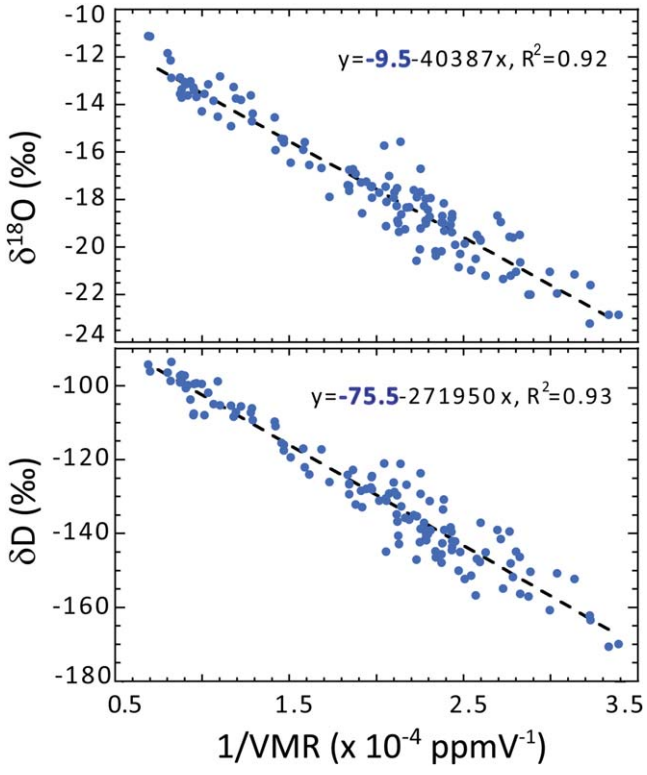

Figure 8. Estimating the isotopic composition of the source moisture by the two source mixing approach [*Keeling*, 1958] using measurements from the Santa Ana episode B period (DOY 40–45). Each data point represents an hourly average. The intercepts are $\delta^{18}O_{source} = -9.5 \pm 0.2‰$ and $\delta D_{source} = -75.5 \pm 1.4‰$.

Keeling intercepts. Many of the *d* values in individual precipitation samples are quite similar to the global average. The precipitation samples collected on DOY 50 have *d* values markedly larger. Interestingly, higher *d* values in atmospheric moisture are also noted on days during and after these rainstorm events (discussed later).

[27] Considering the mean isotope composition of ocean waters and a source of marine vapor in equilibrium with ocean waters, we estimated an isotopic equilibrium temperature c.a. 23°C at the sea surface. This estimate was calculated by inverting the temperature-dependent equilibrium fractionation equation described between liquid and vapor exchange [*Majoube*, 1971]. The key assumption made in this calculation is that kinetic effects associated with evaporation off seawaters are negligible, as indicated by the d_{source} value discussed above. This finding suggests that a great proportion of evaporation fluxes could not have been occurring off the local coastal ocean where the average seawater temperature in February would have been roughly 10°C lower than the apparent isotopic equilibrium temperature. Our estimate suggests that the marine vapor originates from a warmer (likely tropical) ocean that subsequently transported to the coast of southern California by advection, and contributes as a major supply to the atmospheric humidity for this region. This conclusion is consistent with the findings by *Berkelhammer et al*. [2012]. These authors suggested that moisture fluxes advecting across the eastern tropical Pacific are a major source of precipitation in southern California. Their claims were based on findings from significant correlations between moisture fluxes originated in the eastern tropical Pacific and the isotopic composition of precipitation measured over 5 years at four locations in southern California. Our study provides a link between the source of marine moisture fluxes and the isotopic composition of atmospheric water vapor, rather than precipitation, for this region.

[28] The two-source mixing approach yields robust results for the example given above. Nevertheless, when the influence of other processes, such as condensation during rainfall or evapotranspiration [*Lee et al*., 2006], on the isotope ratios becomes important, the mixing approach becomes unreliable. To demonstrate this, we calculated one intercept from the mixing line for each day whenever sufficient data points ($n \geq 10$) were available for the entire study period. Figure 9a shows the coefficient of determination (R^2) for each mixing line, and Figure 9b shows the daily value of the intercept from the mixing line. A predominant mixing process without the complication of condensation (or evapotranspiration) would yield a robust estimate of the δD intercept with a high R^2 value (e.g., > 0.8), which is found to be true for measurements made during the two Santa Ana periods. These results are consistent with the δ-VMR relationship that reveals atmospheric mixing as the dominant control process under the influence of Santa Ana winds as shown in Figure 6. On the other hand, low R^2 values were constantly registered on and following days of a rainstorm event. It is interesting to note that the mixing approach became untenable for an extended time period following the intense rainy period that occurred between DOY 47 and 51. Despite the fair meteorological condition from DOY 52 onward, the processes that control atmospheric humidity remained more complicated than a two-source mixing process would have suggested. We conclude from these results that it is possible to use the Keeling mixing approach to identify conditions when secondary isotopic fractionation processes may be more important than previously thought. Such conditions may be more complex

Table 1. Isotopic Composition of Precipitation Sampled During Two of the Major Rainstorms in San Diego, CA, USA, in February 2011

Day of Year	Hour	$\delta^{18}O$ (‰)	δD (‰)	*d* (‰)
47	16	−3.6	−14.1	14.3
47	17	−3.4	−13.5	13.4
48	0	−2.8	−10.2	12.6
49	16	−2.0	−8.1	7.8
49	17	−5.1	−31.3	9.5
49	19	−6.0	−37.5	10.4
49	19	−5.5	−34.4	9.9
49	21	−5.5	−34.7	9.5
49	22	−7.4	−45.9	13.4
49	23	−7.9	−56.0	7.3
50	0	−7.1	−37.0	19.6
50	15	−4.2	−14.1	19.7
50	15	−8.8	−38.3	31.7
50	22	−9.3	−45.8	28.2
51	6	−9.5	−49.4	26.7
51	7	−6.4	−34.5	16.6

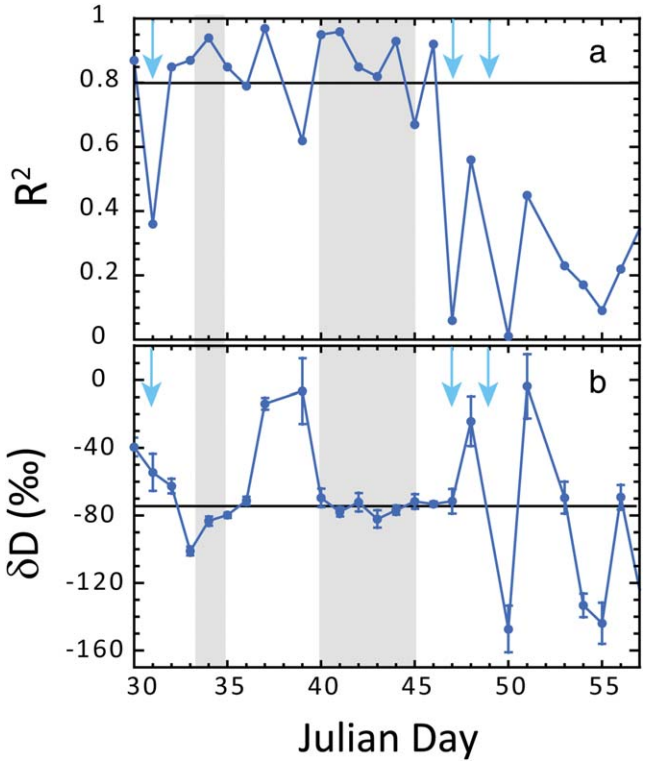

Figure 9. Daily intercepts and significance from the two-source mixing line analysis, including (a) the coefficient of determination (R^2), and (b) the daily δD intercept value, from each mixing line. The two horizontal lines represent a significance threshold (0.8) in Figure 9a and the mean δD intercept value (−75.5‰) for the Santa Ana episode B period in Figure 9b. The blue arrows indicate the timing of the three larger rainstorms whereas the gray boxes indicate the timing of the two Santa Ana wind periods.

than what appears straightforward judging by typical weather classification.

[29] As discussed previously, the average d values increased by nearly 10‰ following two intense rainstorms that began on DOY 47 (Figure 3). One plausible explanation for the observed higher d value is an increased contribution of land evaporation fluxes as a result of a widespread increase in soil moisture contents because of the rainstorms. The IsoGSM simulation shows that latent heat fluxes increased considerably after the two rainstorms (lower plot, Figure 5). Feedbacks from land processes to the atmospheric moisture budget are poorly understood and rarely evaluated in the model. The IsoGSM does not consider the recycling of evapotranspiration fluxes and therefore, it is not surprising that IsoGSM fails to capture the increase in the observed d values following the rainstorms. We suggest that models need to consider these feedback processes, along with the thermodynamics and mixing of air masses, to fully explain the isotopic variability over the continents.

4. Conclusions

[30] (1) Large-scale synoptic weather cycles are a major control of the day-to-day variation in the isotopic composition of atmospheric water vapor at continental sites. The subgrid convection and atmospheric mixing processes further modify this isotopic variation. The influence of evapotranspiration on local atmospheric humidity is detectable by isotope measurements. This evaporative signal is particularly strong at times when large changes in surface wetness occur (i.e., after major rainfalls in a semiarid environment).

[31] (2) The Santa Ana winds represent a unique boundary layer condition in which atmospheric mixing is the dominant process that controls changes in the isotopic composition of water vapor relative to the air humidity. By analyzing the position of isotope data in the δ-VMR space, we were able to separate the control of atmospheric mixing from thermodynamic processes on the isotopic composition of near-surface water vapor.

[32] (3) Using isotope observations and modeling, we demonstrate that atmospheric mixing between dry continental air and moist marine air masses controls the near-surface air humidity in this coastal city in southern California. High-resolution isotope data enable us to estimate the isotopic composition of source moisture on a daily basis. Using this information, we suggest that the transport of marine vapor by advection from a tropical Pacific origin to the coast of southern California represents a major source input to the atmospheric humidity for this region.

[33] (4) This study combines large-scale isotope GCM modeling with a robust and high-resolution isotope data set to disentangle the control of atmospheric and hydrologic processes on the atmospheric humidity in an extratropical climate. Our results demonstrate the power of using single-point, ground-based isotope observations in the study of precipitation and atmospheric moisture cycles. On this basis, we strongly advocate for a coordinated effort to establish a global network of ground-based water vapor isotope measurements at continental sites complimentary to the IAEA's GNIP database.

[34] **Acknowledgments.** The authors thank the U.S. National Science Foundation, Division of Atmospheric and Geospace Sciences, for the funding support under Grant AGS-0956425.

References

Aemisegger, F., P. Sturm, P. Graf, H. Sodemann, S. Pfahl, A. Knohl, and H. Wernli (2012), Measuring variations of δ^{18}O and δ^{2}H in atmospheric water vapour using two commercial laser-based spectrometers: An instrument characterisation study, *Atmos. Meas. Tech.*, *5*(7), 1491–1511.

Araguas-Araguas, L., K. Froehlich, and K. Rozanski (2000), Deuterium and oxygen-18 isotope composition of precipitation and atmospheric moisture, *Hydrol. Process.*, *14*(8), 1341–1355.

Barras, V. and I. Simmonds (2009), Observation and modeling of stable water isotopes as diagnostics of rainfall dynamics over southeastern Australia, *J. Geophys. Res.*, *114*, D23308, doi:10.1029/2009JD012132.

Berkelhammer, M., L. Stott, K. Yoshimura, K. Johnson, and A. Sinha (2012), Synoptic and mesoscale controls on the isotopic composition of precipitation in the western United States, *Clim. Dyn.*, *38*(3–4), 433–454.

Bowen, G. J. and B. Wilkinson (2002), Spatial distribution of δ^{18}O in meteoric precipitation, *Geology*, *30*(4), 315–318.

Brown, D., J. Worden, and D. Noone (2008), Comparison of atmospheric hydrology over convective continental regions using water vapor isotope measurements from space, *J. Geophys. Res.*, *113*, D15124, doi:10.1029/2007JD009676.

Buenning, N. H., L. Stott, K. Yoshimura, and M. Berkelhammer (2012), The cause of the seasonal variation in the oxygen isotopic composition of precipitation along the western U.S. coast, *J. Geophys. Res.*, *117*, D18114, doi:10.1029/2012JD018050.

Ciais, P., and J. Jouzel (1994), Deuterium and oxygen-18 in precipitation—Isotopic model, including mixed cloud processes, *J. Geophys. Res.*, *99*(D8), 16,793–16,803.

Craig, H. (1961), Isotopic variations in meteoric waters, *Science*, *133*, 1702–1703.

Dansgaard, W. (1964), Stable isotopes in precipitation, *Tellus*, *16*(4), 436–468.

Ek, M. B., K. E. Mitchell, Y. Lin, E. Rogers, P. Grunmann, V. Koren, G. Gayno, and J. D. Tarpley (2003), Implementation of Noah land surface model advances in the National Centers for Environmental Prediction operational mesoscale Eta model, *J. Geophys. Res.*, *108*(D22), 8851, doi:10.1029/2002JD003296.

Frankenberg, C., et al. (2009), Dynamic processes governing lower-tropospheric HDO/H_2O ratios as observed from space and ground, *Science*, *325*(5946), 1374–1377.

Galewsky, J., and J. V. Hurley (2010), An advection-condensation model for subtropical water vapor isotopic ratios, *J. Geophys. Res.*, *115*, D16116, doi:10.1029/2009JD013651.

Gat, J. R. (1996), Oxygen and hydrogen isotopes in the hydrologic cycle, *Annu. Rev. Earth Planet. Sci.*, *24*, 225–262.

Good, S. P., K. Soderberg, L. X. Wang, and K. K. Caylor (2012), Uncertainties in the assessment of the isotopic composition of surface fluxes: A direct comparison of techniques using laser-based water vapor isotope analyzers, *J. Geophys. Res*, *117*, D15301, doi:10.1029/2011JD017168.

Griffis, T. J., et al. (2010), Determining the oxygen isotope composition of evapotranspiration using eddy covariance, *Boundary-Layer Meteorol.*, *137*(2), 307–326.

Gupta, P., D. Noone, J. Galewsky, C. Sweeney, and B. H. Vaughn (2009), Demonstration of high-precision continuous measurements of water vapor isotopologues in laboratory and remote field deployments using wavelength-scanned cavity ring-down spectroscopy (WS-CRDS) technology, *Rapid Commun. Mass Spectrom.*, *23*(16), 2534–2542.

Hoffmann, G., M. Werner, and M. Heimann (1998), Water isotope module of the ECHAM atmospheric general circulation model: A study on timescales from days to several years, *J. Geophys. Res.*, *103*(D14), 16,871–16,896.

Hughes, M. and A. Hall (2010), Local and synoptic mechanisms causing Southern California's Santa Ana winds, *Clim. Dyn.*, *34*(6), 847–857.

John, V. O., and B. J. Soden (2007), Temperature and humidity biases in global climate models and their impacts on climate feedbacks, *Geophys. Res. Lett.*, *34*, L18704, doi:10.1029/2007GL030429.

Jouzel, J., G. L. Russell, R. J. Suozzo, R. D. Koster, J. W. C. White, and W. S. Broecker (1987), Simultations of the HDO and H_2O18 atmospheric cycles using the NASA GISS general-circulation model – The seasonal cycle for present-day conditions, *J. Geophys. Res.*, *92*(D12), 14,739–14,760.

Jouzel, J., K. Froehlich, and U. Schotterer (1997), Deuterium and oxygen-18 in present-day precipitation: Data and modelling, *Hydrol. Sci. J.*, *42*(5), 747–763.

Keeling, C. D. (1958), The concentration and isotopic abundances of atmospheric carbon dioxide in rural areas, *Geochim. Et Cosmochim. Acta*, *13*(4), 322–334.

Kendall, C., and T. B. Coplen (2001), Distribution of oxygen-18 and deuterium in river waters across the United States, *Hydrol. Process.*, *15*(7), 1363–1393.

Kurita, N., B. D. Newman, L. J. Araguas-Araguas, and P. Aggarwal (2012), Evaluation of continuous water vapor δD and δ^{18}O measurements by off-axis integrated cavity output spectroscopy, *Atmos. Meas. Tech.*, *5*(8), 2069–2080.

Lai, C. T., and J. Ehleringer (2011), Deuterium excess reveals diurnal sources of water vapor in forest air, *Oecologia*, *165*(1), 213–223.

Lai, C. T., J. R. Ehleringer, B. J. Bond, and K. T. U. Paw (2006), Contributions of evaporation, isotopic non-steady state transpiration and atmospheric mixing on the delta O18 of water vapour in Pacific Northwest coniferous forests, *Plant Cell Environ.*, *29*, 77–94.

Lee, H., R. Smith, and J. Williams (2006), Water vapour 18O/16O isotope ratio in surface air in New England, USA, *Tellus Ser. B*, *58*(4), 293–304.

Lee, J., J. Worden, D. Noone, K. Bowman, A. Eldering, A. LeGrande, J. L. F. Li, G. Schmidt, and H. Sodemann (2011), Relating tropical ocean clouds to moist processes using water vapor isotope measurements, *Atmos. Chem. Phys.*, *11*(2), 741–752.

Lee, X. H., K. Kim, and R. Smith (2007), Temporal variations of the 18O/16O signal of the whole-canopy transpiration in a temperate forest, *Global Biogeochem. Cycles*, *21*, GB3013, doi:10.1029/2006GB002871.

Lee, X., S. D. Sargent, R. B. Smith, and B. Tanner (2005), In situ measurement of the water vapor O-18/O-16 isotope ratio for atmospheric and ecological applications, *J. Atmos. Oceanic Technol.*, *22*, 555–565.

Lee, X., R. Smith, and J. Williams (2006), Water vapour 18O/16O isotope ratio in surface air in New England, USA, *Tellus*, *58*, 293–304.

Majoube, M. (1971), Fractionnement en oxygene 18 et en deuterium entre l'eau et savapeur, *J. Chim. Phys.*, *58*, 1423–1436.

Masson-Delmotte, V., J. Jouzel, A. Landais, M. Stievenard, S. J. Johnsen, J. W. C. White, M. Werner, A. Sveinbjornsdottir, and K. Fuhrer (2005), GRIP deuterium excess reveals rapid and orbital changes of Greenland moisture origin, *Science*, *309*, 118–121.

Merlivat, L., and J. Jouzel (1979), Global climatic interpretation of the deuterium-oxygen-18 relationship for precipitation, *J. Geophys. Res.*, *84*(NC8), 5029–5033.

Noone, D. (2012), Pairing measurements of the water vapor isotope ratio with humidity to deduce atmospheric moistening and dehydration in the tropical midtroposphere, *J. Clim.*, *25*(13), 4476–4494.

Noone, D., et al. (2011), Properties of air mass mixing and humidity in the subtropics from measurements of the D/H isotope ratio of water vapor at the Mauna Loa Observatory, *J. Geophys. Res.*, *116*, D22113, doi:10.1029/2011JD015773.

Pavia, E. G., and A. Badan (1998), ENSO modulates rainfall in the Mediterranean Californias, *Geophys. Res. Lett.*, *25*(20), 3855–3858.

Payne, V. H., D. Noone, A. Dudhia, C. Piccolo, and R. G. Grainger (2007), Global satellite measurements of HDO and implications for understanding the transport of water vapour into the stratosphere, *Q. J. R. Meteorol. Soc.*, *133*(627), 1459–1471.

Pfahl, S., H. Wernli, and K. Yoshimura (2012), The isotopic composition of precipitation from a winter storm—A case study with the limited-area model COSMOiso, *Atmos. Chem. Phys.*, *12*, 1629–1648.

Rambo, J., C.-T. Lai, J. Farlin, M. Schroeder, and K. Bible (2011), On-site calibration for high precision measurements of water vapor isotope ratios using off-axis cavity-enhanced absorption spectroscopy, *J. Atmos. Oceanic Tech.*, *28*(11), 1448–1457.

Risi, C., S. Bony, and F. Vimeux (2008a), Influence of convective processes on the isotopic composition (δ^{18}O and δD) of precipitation and water vapor in the tropics: 2. Physical interpretation of the amount effect, *J. Geophys. Res.*, *113*, D19306, doi:10.1029/2008JD009943.

Risi, C., S. Bony, F. Vimeux, L. Descroix, B. Ibrahim, E. Lebreton, I. Mamadou, and B. Sultan (2008b), What controls the isotopic composition of the African monsoon precipitation? Insights from event-based precipitation collected during the 2006 AMMA field campaign, *Geophys. Res. Lett.*, *35*, L24808, doi:10.1029/2008GL035920.

Risi, C., S. Bony, F. Vimeux, C. Frankenberg, D. Noone, and J. Worden (2010), Understanding the Sahelian water budget through the isotopic composition of water vapor and precipitation, *J. Geophys. Res.*, *115*, D24110, doi:10.1029/2010JD014690.

Rozanski, K., L. Araguasaraguas, and R. Gonfiantini (1992), Relation between long-term trends of O-18 isotope composition of precipitation and climate, *Science*, *258*(5084), 981–985.

Sayres, D. S., L. Pfister, T. F. Hanisco, E. J. Moyer, J. B. Smith, J. M. St Clair, A. S. O'Brien, M. F. Witinski, M. Legg, and J. G. Anderson (2010), Influence of convection on the water isotopic composition of the tropical tropopause layer and tropical stratosphere, *J. Geophys. Res.*, *115*, D00J20, doi:10.1029/2009JD013100.

Schneider, M., K. Yoshimura, F. Hase, and T. Blumenstock (2010), The ground-based FTIR network's potential for investigating the atmospheric water cycle, *Atmos. Chem. Phys.*, *10*(7), 3427–3442.

Sturm, P., and A. Knohl (2010), Water vapor δ^2H and δ^{18}O measurements using off-axis integrated cavity output spectroscopy, *Atmos. Meas. Tech.*, *3*(1), 67–77.

Welp, L. R., X. Lee, K. Kim, T. J. Griffis, K. A. Billmark, and J. M. Baker (2008), δ^{18}O of water vapour, evapotranspiration and the sites of leaf water evaporation in a soybean canopy, *Plant Cell Environ.*, *31*(9), 1214–1228.

Wen, X.-F., S.-C. Zhang, X.-M. Sun, G.-R. Yu, and X. Lee (2010), Water vapor and precipitation isotope ratios in Beijing, China, *J. Geophys. Res.*, *115*, D01103, doi:10.1029/2009JD012408.

Wen, X. F., X. M. Sun, S. C. Zhang, G. R. Yu, S. D. Sargent, and X. Lee (2008), Continuous measurement of water vapor D/H and ^{18}O/^{16}O isotope ratios in the atmosphere, *J. Hydrol.*, *349*(3–4), 489–500.

Worden, J., D. Noone, K. Bowman, and Tropospheric Emission Spectrometer Science Team (2007), Importance of rain evaporation and continental convection in the tropical water cycle, *Nature*, *445*(7127), 528–532.

Worden, J., D. Noone, J. Galewsky, A. Bailey, K. Bowman, D. Brown, J. Hurley, S. Kulawik, J. Lee, and M. Strong (2011), Estimate of bias in Aura TES HDO/H_2O profiles from comparison of TES and in situ HDO/H_2O measurements at the Mauna Loa observatory, *Atmos. Chem. Phys.*, *11*(9), 4491–4503.

Wright, J. S., A. H. Sobel, and G. A. Schmidt (2009), Influence of condensate evaporation on water vapor and its stable isotopes in a GCM, *Geophys. Res. Lett.*, *36*, L12804, doi:10.1029/2009GL038091.

Yoshimura, K., and M. Kanamitsu (2008), Dynamical global downscaling of global reanalysis, *Mon. Weather Rev.*, *136*(8), 2983–2998.

Yoshimura, K., M. Kanamitsu, D. Noone, and T. Oki (2008), Historical isotope simulation using Reanalysis atmospheric data, *J. Geophys. Res.*, *113*, D19108, doi:10.1029/2008JD010074.

Yoshimura, K., M. Kanamitsu, and M. Dettinger (2010), Regional downscaling for stable water isotopes: A case study of an atmospheric river event, *J. Geophys. Res.*, *115*, D18114, doi:10.1029/2010JD014032.

Yoshimura, K., C. Frankenberg, J. Lee, M. Kanamitsu, J. Worden, and T. Röckmann (2011), Comparison of an isotopic atmospheric general circulation model with new quasi-global satellite measurements of water vapor isotopologues, *J. Geophys. Res.*, *116*, D19118, doi:10.1029/2011JD016035.

Zhang, S. C., X. M. Sun, J. L. Wang, G. R. Yu, and X. F. Wen (2011), Short-term variations of vapor isotope ratios reveal the influence of atmospheric processes, *J. Geogr. Sci.*, *21*(3), 401–416. doi:10.1007/s11442-011-0853-6.